Alexandria Engineering Journal (2022) 61, 7843–7851

HOSTED BY

Alexandria University

Alexandria Engineering Journal

www.elsevier.com/locate/aej
www.sciencedirect.com

Soliton theory and modulation instability analysis: The Ivancevic option pricing model in economy

Qiliang Chen [a], **Haci Mehmet Baskonus** [b,*], **Wei Gao** [c], **Esin Ilhan** [d]

[a] *School of Economics and Finance, Chongqing University of Technology, Chongqing, China*
[b] *Faculty of Education, Harran University, Sanliurfa 63050, Turkey*
[c] *School of Information Science and Technology, Yunnan Normal University, Kunming 650500, China*
[d] *Faculty of Engineering and Architecture, Kirsehir Ahi Evran University, 40500 Kirsehir, Turkey*

Received 15 October 2021; revised 20 December 2021; accepted 9 January 2022
Available online 29 January 2022

KEYWORDS

The Ivancevic option pricing model;
RSGEM;
MEFM;
Modulation instability analysis;
Complex;
Mixed dark-bright;
Hyperbolic functions

Abstract In this projected paper, we study on the Ivancevic option pricing model. We apply two important methods, namely, rational sine-Gordon expansion method which is recently developed, and secondly, modified exponential method. Via these methods, we obtain some important properties of Ivancevic option pricing model. We extract many solutions such as complex, periodic, dark bright, mixed dark-bright, singular, travelling and hyperbolic functions. We investigate the option price wave functions of dependent variable, and also, observe the modulation instability analysis in detail. Furthermore, we report the strain conditions for the valid solutions under the family conditions, as well. We simulate the 2D, 3D and counter plots by choosing the suitable values of the parameters involved. Finally, we present the top and low points of pricing in the mentioned intervals via contour simulations.

1. Introduction

In modern century, one of the most studied fields from all over the world is the economy or finance. Developing many technological and scientific tools, experts and scientists produce many more sophisticated products. These devices are used to determine the optimal conditions in all situation of daily life. In this stage of interaction of such devices and its user, they need to know to get maximum benefit or to obtain optimal values. Traditionally, such users choose to use their's current knowledge in determining the values of products. In this case, they come across many different problems coming from buyers, sellers, web platforms, banks, both local and international platforms, as well. Therefore, such problems were studied to explained and investigated by using scientistic norms. Thus, such works introduce more intellectual ways for the user. Therefore, to observe financial market is highly important. Deeper properties of the modeling of a global financial market produce a global informative systems. Especially, these dynamical systems can be used to deep investigation of the productions. Moreover, the transmitting productions from producing to users via various ways such as high way, plane,

* Corresponding author.
E-mail addresses: hmbaskonus@gmail.com (H.M. Baskonus), gaowei@ynnu.edu.cn (W. Gao), eilhan@ahievran.edu.tr (E. Ilhan).
Peer review under responsibility of Faculty of Engineering, Alexandria University.

https://doi.org/10.1016/j.aej.2022.01.029
1110-0168

shipping is one another important points in observing. The first step is to conduct its mathematical models being either complex-valued or real values with wave function. Therefore, many models were developed by experts in extracting their wave distributions in today and future direction. Just at this stage, soliton theory is one of the most used theories because we get exact informations such as periodic, singular, dark, bright, complex and travelling. Such dynamical informations bring an indispensable in understanding, prediction, control and future prospects of complex behaviors of productions. In this sense, Sharp et al. investigated the stochastic differential equations (SDE) in finance [1]. The stability of backward SDE was analyzed under small perturbations of the coefficients and of the boundary values in [2]. They introduced the existence and uniqueness properties. Irving and his team determined the mixed linear-nonlinear coupled differential equations in terms of multivariate discrete time series sequences in [3]. Jin et al. demonstrated the optimal consumption and portfolio rules in a continuous-time finance model in [4]. More recently, fractional order impulsive stochastic differential equation in [5] was studied in controllability by Ganesh and his team. They used the Haar wavelet approximation method to illustrate the theory in numerical integration. In [6], Samarskii introduced the economy splitting schemes. In [7], Decardi-Nelson and their team proposed the robust economic model. They suggested the notion of risk factor in the controller design and provided an algorithm to determine the economic zone to be tracked. Adomian modeled and analyzed a national economy model, namely, coupled nonlinear stochastic multidimensional (discrete or continuous) operator equations by using decomposition method to obtain the solutions of complex dynamical systems [8]. With the developing and advancement of computers, the modelling of large power plants were studied in [9].

Therefore, in modern century, to find deep properties of economy and finance problems by using mathematical models is one of the most studied fields due to its wide application areas of nonlinear science. Such mathematical models are generally presented in the form of nonlinear partial differential equations (NPDEs). One of the most studied NPDEs is the Ivancevic option pricing model (IOPM) given by

$$i\partial_t\Psi(s,t)+\frac{1}{2}\sigma\partial_{ss}\Psi(s,t)+\beta|\Psi(s,t)|^2\Psi(s,t)=0, \tag{1.1}$$

where $i=\sqrt{-1}$, $\Psi(s,t)$ is a complex-valued function of s and t [10]. In Eq. (1.1), the independent variable t being $0\leqslant t<T$ is used to represent time, and s is used to explain the asset price of product and defined $0\leqslant s<\infty$. The dependent variable $\Psi(s,t)$ is used to symbolize the option price wave function. Further, the probability density function is also given by $|\Psi(s,t)|^2$ and this term is used to show the potential field. Furthermore, σ is dispersion frequency coefficient, and it is used to symbolize the volatility being constant or stochastic process itself, (in this paper, it is considered as a constant), and also β is considered as adaptive market potential. Eq. (1.1) is used to describes a nonlinear wave-packet which is defined in the complex-valued wave function. Moreover, Eq. (1.1) presents a relationship among economy and optional pricing. Some properties of Eq. (1.1) are investigated in [11] by using various methods such as trial function method, tanh expansion method, direct perturbation method. In [28], the fractional properties of Ivancevic option pricing model were investigated. In [29], the vector financial wave propagations were extracted. In [30], a nonzero adaptive market potential was studied.

The rest of this paper is organized as follows. In Section 2, two important properties of sine-Gordon equation are obtained. In Section 3, the formulations of methods such as rational sine-Gordon equation (RSGEM) which is recently developed, and modified exponential function method (MEFM) are presented. These two methods are very important for the studied governing model in extracting more deep properties. RSGEM is based on the properties of trigonometric functions. This is the one of the novelties of this paper. Moreover, MEFM is based on the Riccati differential equation. Thus, via these methods, we investigate deeper properties of IOPM in special functions such as trigonometric, periodic, singular, dark, mixed dark-bright, travelling and instability. Moreover, we observe the wave behaviors of IOPM via various simulations. Physically, we extract many different physical features such as price estimation, future direction of any production in economy, determining an increasing trend and so on. In Section 4, the applications of the schemes to the IOPM and the plotted figures are reported. In Section 5, the modulation instability analysis and the stability of the steady state properties are also extracted. In Section 6, novelties and outcomes of this paper are given as a result.

2. Investigation of the sine-Gordon equation

Before starting the main method, we need to extract two important properties of sine-Gordon equation because RSGEM is based on these two important facts coming from sine-Gordon equation given by [12–14]

$$u_{xx}-u_{tt}=m^2\sin(u), \tag{2.1}$$

being m is a real constant and nonzero. With the help of wave transformation given as $u=u(x,t)=U(\xi),\xi=\mu(x-ct)$, Eq. (2.1) may be rewritten as

$$U''=\frac{m^2}{\mu^2(1-c^2)}\sin(U), \tag{2.2}$$

where $U=U(\xi),U''=\frac{d^2U}{d\xi^2}$ and c, μ are real constants nonzero. After some basic calculations, Eq. (2.2) may be rewritten as

$$\left(\left(\frac{U}{2}\right)'\right)^2=\frac{m^2}{\mu^2(1-c^2)}\sin^2\left(\frac{U}{2}\right)+k, \tag{2.3}$$

being k is an integral constant. Considering as $k=0,\ \omega=\frac{U}{2}$, and $a^2=\frac{m^2}{\mu^2(1-c^2)}$, Eq. (2.3) reads as

$$\omega'=a\sin(\omega), \tag{2.4}$$

in which $\omega=\omega(\xi)$. Putting as $a=1$ and solving yields the following two important properties as [16,17]

$$\sin(\omega)=\frac{2pe^{\xi}}{p^2e^{2\xi}+1}\downarrow p_{=1}=\mathrm{sech}(\xi), \tag{2.5}$$

$$\cos(\omega)=\frac{2pe^{\xi}}{p^2e^{2\xi}+1}\downarrow p_{=1}=\tanh(\xi). \tag{2.6}$$

3. Formulations of schemes

3.1. Projected RSGEM

This part presents the general properties of RSGEM which is newly developed scheme. Let's start the general nonlinear mathematical model given as

$$P(\Xi, \Xi_x, \Xi_{xt}, \Xi^2, \cdots) = 0. \tag{3.1}$$

In Eq. (3.1) when we apply the wave transformation as $\Xi = \Xi(x,t) = U(\xi), \xi = \mu(x - ct)$, we convert Eq. (3.1) into the following nonlinear differential equation given by

$$N(U, U', U'', U^2, \cdots) = 0. \tag{3.2}$$

where $U = U(\xi), U' = \frac{dU}{d\xi}$. In Eq. (3.2), we suppose the test function of solution formula as

$$U = \frac{\sum_{i=1}^{n} \tanh^{i-1}(\xi)[A_i \mathrm{sech}(\xi) + c_i \tanh(\xi)] + A_0}{\sum_{i=1}^{M} \tanh^{i-1}(\xi)[B_i \mathrm{sech}(\xi) + d_i \tanh(\xi)] + B_0}. \tag{3.3}$$

With the help of Eqs. (2.5) and (2.6), Eq. (3.3) is rewritten as

$$U = \frac{\sum_{i=1}^{n} \cos^{i-1}(\omega)[A_i \sin(\omega) + c_i \cos(\omega)] + A_0}{\sum_{i=1}^{M} \cos^{i-1}(\omega)[B_i \sin(\omega) + d_i \cos(\omega)] + B_0}. \tag{3.4}$$

Balancing in Eq. (3.2), we find the relationship between n and M producing the analytical solution to the Eq. (3.1).

3.2. Projected MEFM

In this subsection, we present the general properties of MEFM. Let's start the general nonlinear mathematical model given as

$$P(\Psi, \Psi_x, \Psi_{xt}, \Psi^2, \cdots) = 0.$$

In this equation, when we apply the wave transformation as $\Psi = \Psi(x,t) = \mathrm{U}(\xi), \xi = \mu(x - ct)$, it produces

$$N(\mathrm{U}, \mathrm{U}', \mathrm{U}'', \mathrm{U}^2, \cdots) = 0.$$

where $\mathrm{U} = \mathrm{U}(\xi), U' = \frac{d\mathrm{U}}{d\xi}$. In this last equation, we suppose the test function of solution formula as

$$\mathrm{U} = \frac{\sum_{i=0}^{N} A_i [e^{-\Omega}]^i}{\sum_{j=0}^{M} B_j [e^{-\Omega}]^j} = \frac{A_0 + A_1 e^{-\Omega} + \cdots + A_N e^{-N\Omega}}{B_0 + B_1 e^{-\Omega} + \cdots + B_M e^{-M\Omega}}, \tag{3.5}$$

where $A_i, B_j, (0 < i \leqslant N, 0 < j \leqslant M)$ are constants to be determined later. In Eq. (3.5) $\Omega = \Omega(\xi)$ satisfies the following differential equation

$$\Omega' = exp(-\Omega) + \mu exp(\Omega) + \lambda. \tag{3.6}$$

Eq. (3.6) is of the following several families [15,18,19]

Family 1: When $\mu \neq 0, \lambda^2 - 4\mu > 0$,

$$\Omega(\xi) = ln\left(\frac{-\sqrt{\lambda^2 - 4\mu}}{2\mu} \times \tanh\left(\frac{\sqrt{\lambda^2 - 4\mu}}{2}(\xi + E)\right) - \frac{\lambda}{2\mu}\right). \tag{3.7}$$

Family 2: When $\mu \neq 0, \lambda^2 - 4\mu < 0$,

$$\Omega(\xi) = ln\left(\frac{\sqrt{-\lambda^2 + 4\mu}}{2\mu} \times \tan\left(\frac{\sqrt{-\lambda^2 + 4\mu}}{2}(\xi + E)\right) - \frac{\lambda}{2\mu}\right). \tag{3.8}$$

Family 3: When $\mu = 0, \lambda \neq 0$ and $\lambda^2 - 4\mu > 0$,

$$\Omega(\xi) = -ln\left(\frac{\lambda}{e^{\lambda(\xi+E)} - 1}\right). \tag{3.9}$$

Family 4: When $\mu \neq 0, \lambda \neq 0$ and $\lambda^2 - 4\mu = 0$,

$$\Omega(\xi) = ln\left(-\frac{2\lambda(\xi + E) + 4}{\lambda^2(\xi + E)}\right). \tag{3.10}$$

Family 5: When $\mu = 0, \lambda = 0$ and $\lambda^2 - 4\mu = 0$,

$$\Omega(\xi) = ln(\xi + E). \tag{3.11}$$

$A_i, B_j, (0 \leqslant i \leqslant N, 0 \leqslant j \leqslant N), E, \lambda, \mu$ are coefficients to be obtained, and M, N are positive integers that one can find by the balancing principle.

Step 3: Inserting Eq. (3.5) into Eq. (3.2) produces new solutions to the Eq. (3.1).

4. Applications

This section applies these two powerful schemes in extracting the periodic, complex, dark, travelling wave and other solutions to Eq. (1.1).

4.1. Application of the RSGEM

Taking the following travelling wave transformation given by

$$\Psi(s,t) = U(\xi)e^{i\psi}, \ \xi = \tau t + \rho s, \ \psi = wt + \kappa s, \tag{4.1}$$

where τ and w are time velocity, and ρ and κ are the parameters coming from the asset price of product. Substituting Eq. (4.1) into Eq. (1.1), yields

$$\rho^2 \nabla \mathrm{U} - (\kappa^2 + 2w)\mathrm{U} + 2\beta \mathrm{U}^3 = 0, \tag{4.2}$$

from the real part while we obtain the following equality from the imaginary part

$$\tau + \kappa\rho = 0 \Rightarrow \tau = -\rho\kappa, \tag{4.3}$$

where $\nabla(.) = \frac{d^2(.)}{d\xi^2}$. Eq. (4.3) is one of the important steps obtained from complex dynamic. Due to Eq. (4.3), the governing model render to apply RSGEM and MEFM. Specially, considering as $M = 1$ and $n = 1$ into Eq. (3.4), we get the following test function of the solution formula for Eq. (4.2)

$$\mathrm{U} = \frac{A_0 + A_1 \sin(\omega) + c_1 \cos(\omega)}{B_0 + B_1 \sin(\omega) + d_1 \cos(\omega)}. \tag{4.4}$$

Putting Eq. (4.4) into (4.2) presents an algebraic equations of trigonometric functions. By calculating via various programs, we find the values of $A_0, A_1, B_0, B_1, \beta, \kappa, w, \rho, d_1, c_1$.

Set-1: When $A_0 = \frac{\sqrt{A_1^2+c_1^2}d_1}{\sqrt{B_1^2+d_1^2}}, B_0 = \frac{c_1\sqrt{B_1^2+d_1^2}}{\sqrt{A_1^2+c_1^2}}, \rho = \frac{2\sqrt{-\beta(A_1^2+c_1^2)}}{\sqrt{B_1^2+d_1^2}}$, $w = -\frac{\kappa^2}{2} + \frac{\beta(A_1^2+c_1^2)}{B_1^2+d_1^2}$, we have the mixed dark-bright travelling wave soliton as

$$\Psi_{1,1} = e^{i(\kappa s + t\varsigma)} \times \frac{A_1 \mathrm{sech}(2sv - 2t\kappa v) + \frac{\sqrt{A_1^2+c_1^2}d_1}{\sqrt{B_1^2+d_1^2}} + c_1 \tanh(2sv - 2t\kappa v)}{B_1 \mathrm{sech}(2sv - 2t\kappa v) + \frac{\sqrt{B_1^2+d_1^2}c_1}{\sqrt{A_1^2+c_1^2}} + d_1 \tanh(2sv - 2t\kappa v)}, \tag{4.5}$$

where $\varsigma = -\frac{\kappa^2}{2} + \frac{\beta(A_1^2+c_1^2)}{B_1^2+d_1^2}, v = \frac{\sqrt{-\beta(A_1^2+c_1^2)}}{\sqrt{B_1^2+d_1^2}}$,and $\beta < 0$ for valid solitons.

Remark-1 In the solution $\Psi_{1.1}(s,t)$ is $A_1 \neq B_1$ and $c_1 \neq d_1$, simultaneously, for valid solution. **Set-2:** If $A_0 = \frac{c_1 d_1}{B_0}$, $A_1 = \frac{ic_1\sqrt{B_0^2-B_1^2-d_1^2}}{B_0}$ $\kappa = -\sqrt{\frac{-\rho^2}{2} - 2w}$, $\beta = -\frac{\rho^2 B_0^2}{4c_1^2}$,we have the mixed complex dark-bright solution as

$$\Psi_{1.2} = \frac{c_1}{B_0} e^{i(-s\zeta + tw)} \times \frac{d_1 + i\text{sech}(s\rho + t\rho\zeta)\vartheta + B_0 \tanh(s\rho + t\rho\zeta)}{B_0 + B_1 \text{sech}(s\rho + t\rho\zeta) + d_1 \tanh(s\rho + t\rho\zeta)}, \quad (4.6)$$

where $\zeta = \sqrt{\frac{-\rho^2}{2} - 2w}, \vartheta = \sqrt{B_0^2 - B_1^2 - d_1^2}$, and, $B_0^2 - B_1^2 - d_1^2 > 0$, $\frac{-\rho^2}{2} - 2w > 0$,for valid solitons.

Set-3: It is selected as $A_0 = \frac{c_1 d_1}{B_0}$, $A_1 = -\frac{ic_1\sqrt{B_0^2-B_1^2-d_1^2}}{B_0}$, $\kappa = -\sqrt{\frac{-\rho^2}{2} - 2w}$, $\beta = -\frac{\rho^2 B_0^2}{4c_1^2}$,we have conjugate solution in mixed dark-bright given as as

$$\Psi_{1.3} = \frac{c_1}{B_0} e^{i(-s\zeta + tw)} \frac{d_1 - i\text{sech}(s\rho + t\rho\zeta)\vartheta + B_0 \tanh(s\rho + t\rho\zeta)}{B_0 + B_1 \text{sech}(s\rho + t\rho\zeta) + d_1 \tanh(s\rho + t\rho\zeta)}, \quad (4.7)$$

where $\zeta = \sqrt{\frac{-\rho^2}{2} - 2w}, \vartheta = \sqrt{B_0^2 - B_1^2 - d_1^2}$, and, $B_0^2 - B_1^2 - d_1^2 > 0$, $\frac{-\rho^2}{2} - 2w > 0$,for valid solitons.

Set-4: Taken as $A_0 = \frac{-i\rho d_1}{2\sqrt{\beta}}$, $A_1 = \frac{\sqrt{-4\beta c_1^2 - \rho^2(B_1^2+d_1^2)}}{2\sqrt{\beta}}$, $B_0 = \frac{2i\sqrt{\beta}c_1}{\rho}$, $w = \frac{1}{4}(-2\kappa^2 - \rho^2)$, $\tau = -\kappa\rho$produces another mixed soliton solution

$$\Psi_{1.4} = \frac{\rho e^{i(s\kappa + wt)}(-i\rho d_1 + \sqrt{\hbar}\text{sech}(\rho s - \kappa\rho t) + 2\sqrt{\beta}c_1 \tanh(\rho s - \kappa\rho t))}{2\sqrt{\beta}(\rho B_1 \text{sech}(\rho s - \kappa\rho t) + 2i\sqrt{\beta}c_1 + \rho d_1 \tanh(\rho s - \kappa\rho t))}, \quad (4.8)$$

where $\hbar = -4\beta c_1^2 - \rho^2(B_1^2 + d_1^2)$, and, $\hbar > 0$for valid solitons.

4.2. Application of the MEFM

Balancing the terms U'' and U^3 in Eq. (4.2), we get the relation; $N = M + 1$. Choosing $M = 1$, and $N = 2$ Eq. (3.5), becomes

$$U(\xi) = \frac{A_0 + A_1 e^{-\Omega(\xi)} + A_2 e^{-2\Omega(\xi)}}{B_0 + B_1 e^{-\Omega(\xi)}}. \quad (4.9)$$

Substituting Eq. (4.9) along with Eq. (3.6), yields a polynomial in powers of exponential functions which produces the values of the parameters involved into different cases.

Case-1: When $A_0 = \frac{i\lambda\rho B_0}{2\sqrt{\beta}}, A_1 = \frac{i\rho(2B_0+\lambda B_1)}{2\sqrt{\beta}}; A_2 = \frac{i\rho B_1}{\sqrt{\beta}}, w = -\frac{\kappa^2}{2} - \frac{1}{4}(\lambda^2 - 4\mu)\rho^2$, we get the following mixed dark soliton solution

$$\Psi_{1.5} = \frac{ie^{i\left(s\kappa + t\left(-\frac{\kappa^2}{2} - \frac{1}{4}\sqrt{\chi}\rho^2\right)\right)}\mu\rho\left(2 + \frac{\lambda\left(-\lambda - \sqrt{\chi}\text{Tanh}\left[\frac{1}{2}\sqrt{\chi}(\text{E} + s\rho - t\kappa\rho)\right]\right)}{2\mu}\right)}{\sqrt{\beta}\left(-\lambda - \sqrt{\chi}\text{Tanh}\left[\frac{1}{2}\sqrt{\chi}(\text{E} + s\rho - t\kappa\rho)\right]\right)}, \quad (4.10)$$

where $\chi = \lambda^2 - 4\mu$, under the terms of *family-1* being $\mu \neq 0, \lambda^2 - 4\mu > 0$ for validity solution.

Case-2: Once it is selected as $A_0 = -\frac{i\lambda\rho B_0}{2\sqrt{\beta}}, A_1 = -\frac{i\rho(2B_0+\lambda B_1)}{2\sqrt{\beta}}$, $A_2 = -\frac{i\rho B_1}{\sqrt{\beta}}, w = -\frac{\kappa^2}{2} - \frac{1}{4}(\lambda^2 - 4\mu)\rho^2$, we extract the complex conjugate of $\Psi_{1.5}$ as

$$\Psi_{1.6} = -\frac{i\mu\rho e^{i(\kappa s + jt)}\left(2 + \frac{\lambda}{2\mu}\left(-\lambda - \sqrt{\chi}\tanh\left(\frac{1}{2}\sqrt{\chi}(\text{E} + s\rho - t\kappa\rho)\right)\right)\right)}{\sqrt{\beta}\left(-\lambda - \sqrt{\chi}\tanh\left(\frac{1}{2}\sqrt{\chi}(\text{E} + s\rho - t\kappa\rho)\right)\right)}, \quad (4.11)$$

being $\chi = \lambda^2 - 4\mu, j = -\frac{\kappa^2}{2} - \frac{1}{4}\chi\rho^2$.

Case-3: Taken as $B_0 = \frac{\lambda A_0 B_1}{-2A_0 + \lambda A_1}, \beta = -\frac{\lambda^4\rho^2 B_1^2}{4(-2A_0+\lambda A_1)^2}$, $A_2 = \frac{2(-2A_0+\lambda A_1)}{\lambda^2}, w = -\frac{\kappa^2}{2} - \frac{1}{4}(\lambda^2 - 4\mu)\rho^2$, extracts the dark soliton solution

$$\Psi_{1.7} = \frac{\hbar e^{i(\kappa s + \varrho t)}\left(2 - \frac{\lambda}{2\mu}\left(\lambda + \varsigma\tanh\left[\frac{1}{2}\varsigma(\text{E} + s\rho - t\kappa\rho)\right]\right)\right)}{\lambda^2 B_1\left(-\lambda - \varsigma\tanh\left[\frac{1}{2}\varsigma(\text{E} + s\rho - t\kappa\rho)\right]\right)}, \quad (4.12)$$

being $\hbar = 2\mu(-2A_0 + \lambda A_1), \varrho = -\frac{\kappa^2}{2} - \frac{1}{4}(\lambda^2 - 4\mu)\rho^2, \varsigma = \sqrt{\lambda^2 - 4\mu}$.

Case-4: Under the *family-1* conditions, considered as $A_0 = \frac{1}{2}i(\lambda^2 - 2\mu), A_1 = i\lambda, B_1 = \frac{2B_0}{\lambda}, w = -\frac{\kappa^2}{2} + \frac{\beta\left(-\frac{\lambda^4}{4}+\lambda^2\mu\right)}{B_0^2}, \rho = \frac{\sqrt{\beta}\lambda}{2B_0}$, $A_2 = i$, produces another new dark soliton solution

$$\Psi_{1.8} = \frac{ie^{if(s,t)}\lambda\mu\left(2 + \frac{\lambda}{\mu}(-\lambda - \hbar\tanh(g(s,t))) - \frac{\Xi}{4\mu^2}[\lambda + \hbar\tanh(g(s,t))]^2\right)}{B_0[-\lambda - \hbar\tanh(g(s,t))][2 + \imath(-\lambda - \hbar\tanh(g(s,t)))]}, \quad (4.13)$$

being $f(s,t) = s\kappa + t(-\frac{\kappa^2}{2} + \frac{\beta}{B_0^2}(-\frac{\lambda^4}{4} + \lambda^2\mu)), g(s,t) = \frac{1}{2}\hbar\left(\text{E} + \frac{s\sqrt{\beta}\lambda}{2B_0} - \frac{t\sqrt{\beta}\kappa\lambda}{2B_0}\right), \hbar = \sqrt{\lambda^2 - 4\mu}, \Xi = \lambda^2 - 2\mu, \imath = \frac{\lambda}{2\mu}$.

Case-5: With the help of *family-1* conditions, taken as $A_0 = -i(\lambda^2 - 2\mu), A_1 = -2i\lambda; B_1 = \frac{2B_0}{\lambda}, \beta = -\frac{(\kappa^2+2w)B_0^2}{2\lambda^2(\lambda^2-4\mu)}, \rho = -\frac{\sqrt{-\kappa^2-2w}}{\sqrt{2}\sqrt{\lambda^2-4\mu}}$, $A_2 = -2i$, we find the periodic solution as

$$\Psi_{1.9} = -\frac{ie^{i(s\kappa + tw)}j\left(\phi - \theta\hbar\tanh(f(s,t)) - \wp(\lambda + \hbar\tanh(f(s,t)))^2\right)}{B_0(-\lambda - \hbar\tanh(f(s,t)))\left(2 + \frac{\lambda(-\lambda - \hbar\tanh(f(s,t)))}{2\mu}\right)}, \quad (4.14)$$

being $f(s,t) = \frac{1}{2}\hbar(\text{E} - \frac{s\sqrt{-\kappa^2-2w}}{\sqrt{2}\hbar} + \frac{t\kappa\sqrt{-\kappa^2-2w}}{\sqrt{2}\hbar}), \hbar = \sqrt{\lambda^2 - 4\mu}$, $j = 2\lambda\mu, \wp = \frac{\lambda^2-2\mu}{4\mu^2}, \theta = \frac{\lambda}{\mu}, \phi = 2 - \theta\lambda$.

5. Modulation instability analysis

In this part of the study, modulation instability analysis (MI) for the stationary solutions of Eq. (1.1) is studied by supposing that Eq. (1.1) have the following stationary solution

$$\chi(s,t) = (\sqrt{a_0} + \Psi(s,t))e^{-ia_0 s}, \quad (5.1)$$

where a_0 represent the incident power. We investigate the evolution of the perturbation $\Psi(s,t)$ using the concept of linear stability analysis. Substituting Eq. (5.1) into Eq. (1.1) and linearizing the result in $\Psi(s,t)$, we acquire

$$i\Psi_t + \frac{\sigma}{2}\Psi_{ss} + \beta a_0(\Psi + \Psi^*) = 0, \quad (5.2)$$

where Ψ^* is the conjugate function and σ is dispersion frequency coefficient, supposing solutions of Eq. (5.2) are in the following format

$$\Psi(s,t) = \gamma e^{i(\beta s-\alpha t)} + \delta e^{-i(\beta s-\alpha t)}, \tag{5.3}$$

where β is the wave number, α is the frequency of the perturbation. Putting Eq. (5.3) into Eq. (5.2) gives a set of two homogenous equations as follows

$$\begin{aligned} &-\alpha\gamma - \tfrac{1}{2}\beta^2\gamma\sigma + \beta\gamma a_0 + \beta\tau a_0 = 0 \\ &\alpha\tau - \tfrac{1}{2}\beta^2\sigma\tau + \beta\gamma a_0 + \beta\tau a_0 = 0. \end{aligned} \tag{5.4}$$

From Eq. (5.4), one can easily obtain the following coefficient matrix of γ and τ

$$\begin{pmatrix} -\alpha - \frac{1}{2}\beta^2\sigma + \beta a_0 & \beta a_0 \\ \beta a_0 & \alpha - \frac{1}{2}\beta^2\sigma + \beta a_0 \end{pmatrix} \begin{pmatrix} \gamma \\ \tau \end{pmatrix} = \begin{pmatrix} 0 \\ 0 \end{pmatrix}. \tag{5.5}$$

The coefficient matrix in Eq. (5.5) has a nontrivial solution if the determinant equal to zero. By expanding the determinant, we obtain the following

$$-\alpha^2 + \frac{\beta^4\sigma^2}{4} - \beta^3\sigma a_0 = 0, \tag{5.6}$$

Eq. (5.6) has the following solutions for α :

$$\begin{aligned} \alpha &= \tfrac{1}{2}\beta^{3/2}\sqrt{\sigma}\sqrt{\beta\sigma - 4a_0} \\ \alpha &= -\tfrac{1}{2}\beta^{3/2}\sqrt{\sigma}\sqrt{\beta\sigma - 4a_0}. \end{aligned} \tag{5.7}$$

The stability of the steady state is determined by Eq. (5.7), when α has an imaginary part. Thus, the necessary condition necessary for the existence of modulation instability to occur from Eq. (5.8) is when either

$$\beta\sigma - 4a_0 > 0, \ \textit{and}\ \sigma < 0, \tag{5.8}$$

or

$$\beta\sigma - 4a_0 < 0, \ \textit{and}\ \sigma > 0. \tag{5.9}$$

Now for investigating instability modulation gain spectrum it should be noted that

$$g(\beta) = 2Im(\alpha) = \mp\beta^{3/2}\sqrt{\sigma}\sqrt{\beta\sigma - 4a_0}, \tag{5.10}$$

we have the following cases,

Case-1 If it is considered as

$$g(\beta) = 2Im(\alpha) = -\beta^{3/2}\sqrt{\sigma}\sqrt{\beta\sigma - 4a_0}, \tag{5.11}$$

we have the following sub-cases

Case 1.1) For these values $a_0 = 1, \sigma = \frac{1}{3}$ we have

$$g_{1.1}(\beta) = -\frac{1}{3}\beta^{3/2}\sqrt{\beta - 12}.$$

Case 1.2) For these values $a_0 = -1, \sigma = 2$ we have

$$g_{1.2}(\beta) = -2\beta^{3/2}\sqrt{\beta + 2}.$$

Case 1.3) When $a_0 = \frac{1}{4}, \sigma = 1$ we have

$$g_{1.3}(\beta) = -\beta^{3/2}\sqrt{\beta - 1}.$$

Case 1.4) When we consider these parameters given as $a_0 = -\frac{1}{5}, \sigma = \frac{1}{2}$ we have

$$g_{1.4}(\beta) = -\frac{1}{2}\beta^{3/2}\sqrt{\beta + \frac{8}{5}}.$$

Case-2 When it is selected as

$$g(\beta) = 2Im[\alpha] = \beta^{3/2}\sqrt{\sigma}\sqrt{\beta\sigma - 4a_0}, \tag{5.12}$$

we have the following sub-cases

Case 2.1) For these values $a_0 = 1, \sigma = \frac{1}{4}$ we have

$$g_{2.1}(\beta) = \frac{1}{4}\beta^{3/2}\sqrt{-16 + \beta}.$$

Case 2.2) For these values $a_0 = -1, \sigma = 2$ we have

$$g_{2.2}(\beta) = 2\beta^{3/2}\sqrt{\beta + 2}.$$

Case 2.3) Once $a_0 = \frac{1}{9}, \sigma = 1$ we have

$$g_{2.3}(\beta) = \beta^{3/2}\sqrt{\beta - \frac{4}{9}}.$$

Case 2.4) When $a_0 = -1, \sigma = \frac{1}{2}$ we have

$$g_{2.4}(\beta) = \frac{1}{2}\beta^{3/2}\sqrt{\beta + 8}.$$

Case 2.5) If $a_0 = \frac{1}{9}, \sigma = \frac{1}{5}$ we have

$$g_{2.5}(\beta) = \frac{1}{15}\beta^{3/2}\sqrt{-20 + 9\beta}.$$

These sub-cases can be expressed as the following graphs

6. Results and discussion

In this part of the paper, we present some remarks and physical meanings of figures. All figures were plotted under the suit-

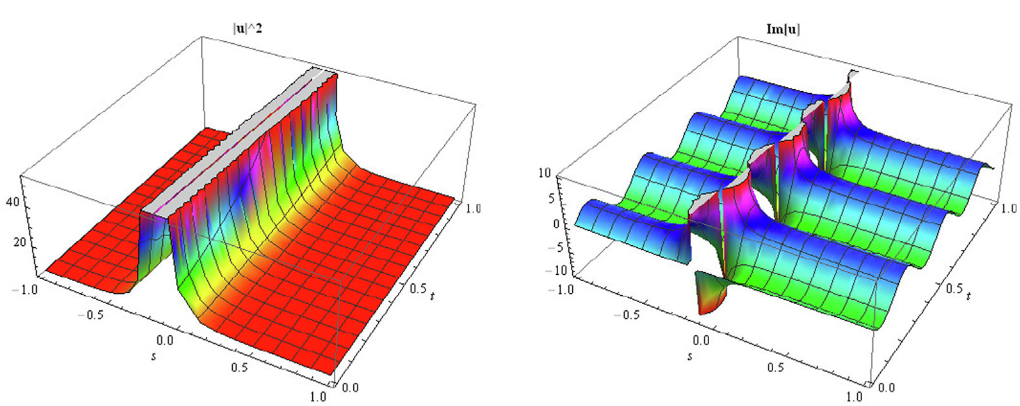

Fig. 1 The 3D surfaces of Eq. (4.5) under the values, $\kappa = 0.1,\ \beta = -3,\ A_1 = 0.5,\ c_1 = 0.3,\ B_1 = .0.1,\ d_1 = 0.2.$

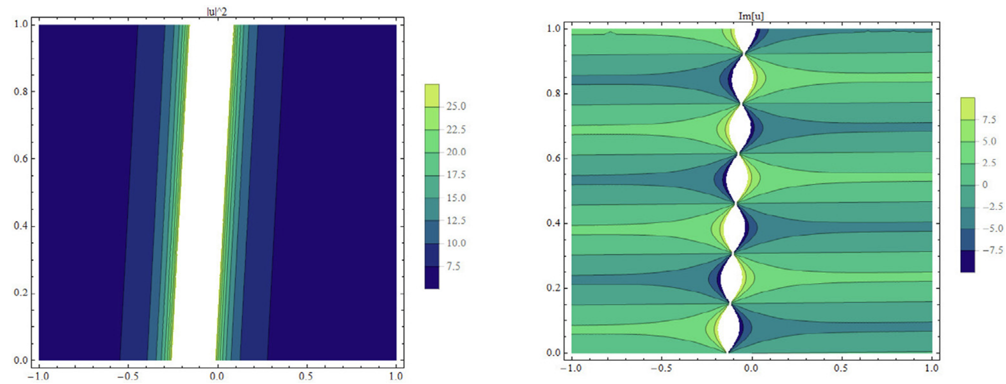

Fig. 2 The contour surfaces of Eq. (4.5) under the values $\kappa = 0.1,\ \beta = -3,\ A_1 = 0.5,\ c_1 = 0.3,\ B_1 = .0.1,\ d_1 = 0.2.$

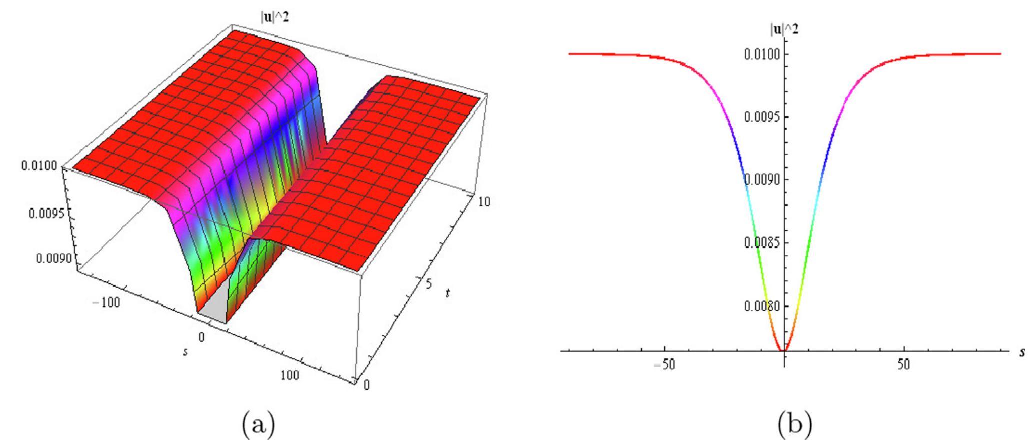

Fig. 3 The (a) 3D surface and (b) 2D surface of Eq. (4.6) under the values, $\rho = 0.1,\ w = -0.3,\ B_0 = 3,\ c_1 = 0.3,\ B_1 = 0.4,\ d_1 = 0.2.$ and $t = 0.123.$ for 2D graph.

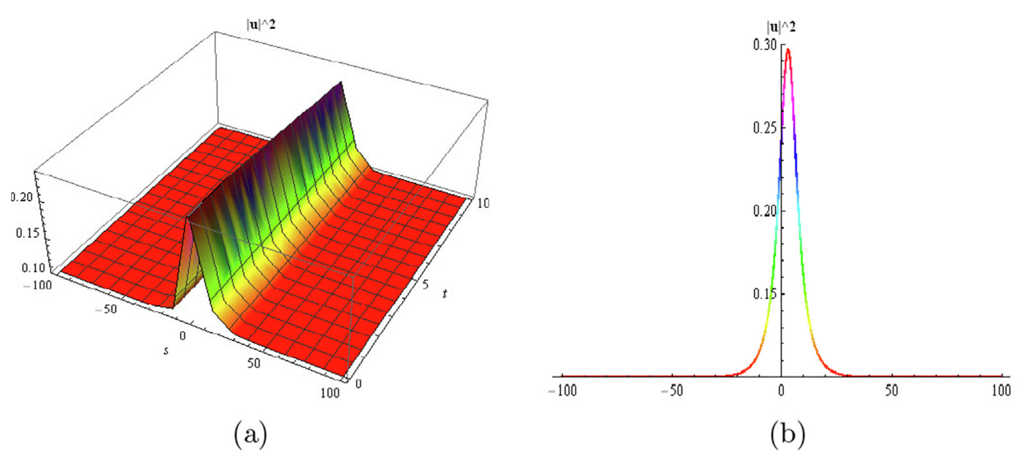

Fig. 4 The (a) 3D surface and (b) 2D surface of Eq. (4.8) under the values, $\kappa = 0.1,\ \beta = -0.1,\ \rho = 0.2,\ B_1 = 0.4,\ d_1 = 0.5,\ c_1 = 0.3,$ and $t = 0.12$ for 2D graph.

able values of the parameters. Fig. 1 is used to symbolize the mixed dark-bright simulation. Its fluctuation is also seen in the right side via imaginary part. In Fig. 2, the high and low points of these fluctuations are also observed in contour simulations. Figs. 3 and 4 are another singular simulation which the governing model is stable. Fig. 5 explain another wave

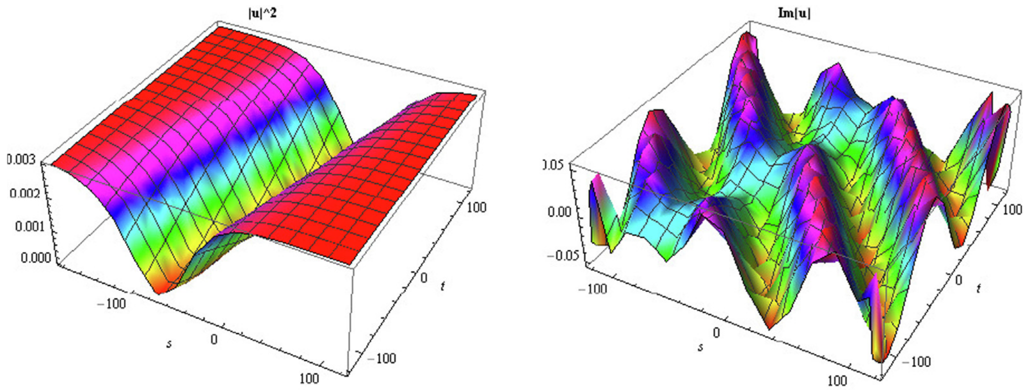

Fig. 5 The 3D surfaces of Eq. (4.10) under the values, $\lambda = 0.8,\ \mu = 0.1,\ E = 0.5,\ \kappa = 0.3,\ \rho = 0.1,\ \beta = 0.2$.

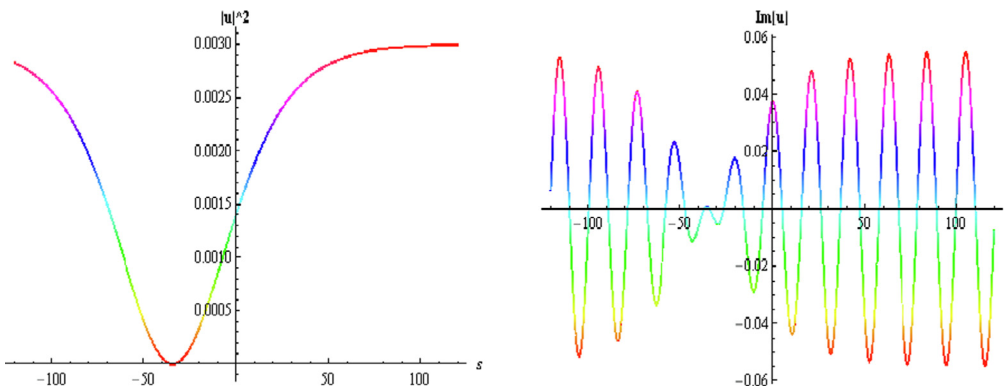

Fig. 6 The 2D surfaces of Eq. (4.10) under the values, $\lambda = 0.8,\ \mu = 0.1,\ E = 0.5,\ \kappa = 0.3,\ \rho = 0.1,\ \beta = 0.2, t = 0.11$.

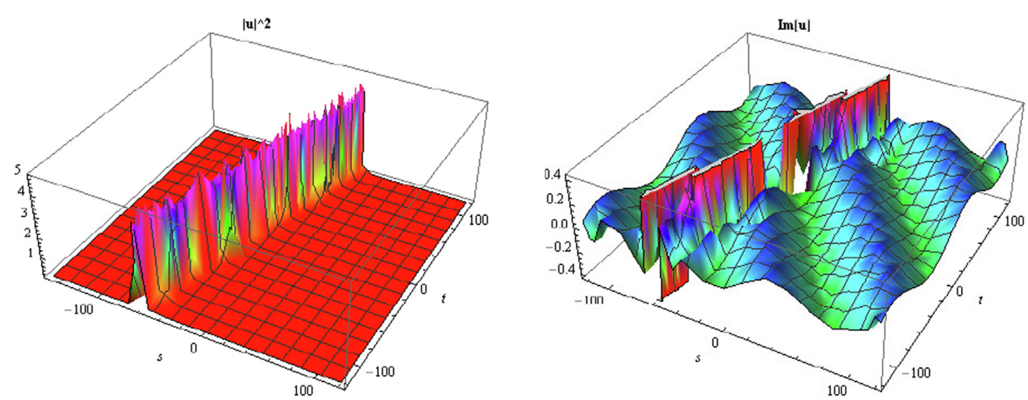

Fig. 7 The 3D surfaces of Eq. (4.11) under the values $\lambda = 0.8,\ \mu = -0.1,\ E = 0.5,\ \kappa = 0.3,\ \rho = 0.1,\ \beta = 0.2$.

distribution of governing model in mixed dark-bright soliton solution. Fig. 6 is two dimensional simulation for $t = 0.11$. Fig. 7 is strict singular wave simulation which is coming from the strain condition of *Family* − 1. Fig. 8 is used to plot in a wide range. In this figure, wave fluctuations of IOPM are simulated in frequent. Fig. 9 is plotted to show the stability range of the parameters of IOPM. This is very important the test function of the solution formula for valid result.

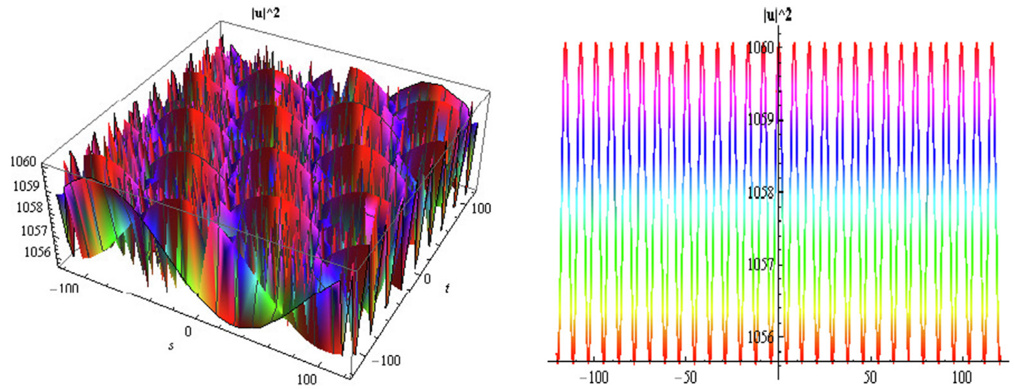

(a) (b)

Fig. 8 The (a) 3D surface (b) 2D surface of Eq. (4.14) under the values $\lambda = 2$, $\mu = 0.2$, $E = 0.5$, $\kappa = 0.3$, $w = 0.1$, $B_0 = 0.11$ and $t = 0.13$ for 2D graph.

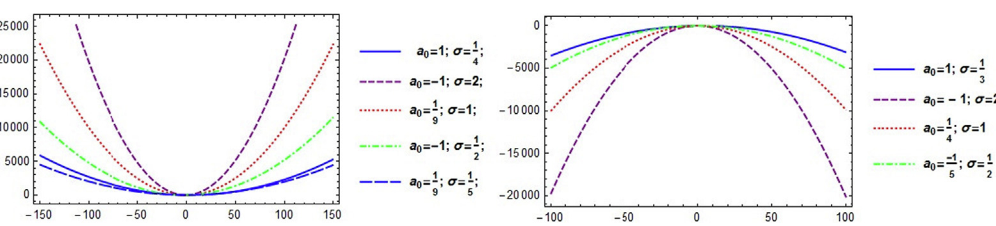

Fig. 9 The modulation instability graphs for different values in Eqs. (5.11) and (5.12).

7. Conclusions

In this article, RSGEM and MEFM were successfully applied to the governing model in extracting the dark, complex, mixed dark-bright, singular solitons, periodic and trigonometric functions solutions to IOPM. The instability modulation analysis for the stationary solution of Eq. (1.1) is investigated. The constraint conditions are reported in detail. Choosing suitable values of parameters the two-dimensional and three-dimensional surfaces were plotted via computational programs. The direction of the option price wave function's in the future may be estimated by these findings such as singular from the figures and contour points. From Fig. 9 plotted via instability modulation analysis, it is concluded that an adaptive market potential is closely related to the representation of the incident power and the dispersion frequency coefficient, a_0 and σ, respectively [20–27]. The extracted results may be used to explain some deeper properties of IOPM economy model. Their option price wave fluctuations are given with the real physical meanings of IOPM economy model and stable option price pulses. All the acquired solutions of the IOPM model have numerous applications in many branches of nonlinear sciences, including economy, finance, the option price and so on. For example, the sine-Gordon traveling waves can give new insights in determining and controlling the option price wave fluctuation of long time assets of productions. Thus, RSGEM which recently developed method and MEFM may be also used to find different solutions of nonlinear model arising in the field of economy and other related fields [31–42].

Availability of data and materials

Data sharing is not applicable to this paper as no datasets were generated or analyzed during the current study.

Ethics approval and consent to participate

Authors declare that there is not any ethical approval.

Declaration of Competing Interest

The authors declare that they have no known competing financial interests or personal relationships that could have appeared to influence the work reported in this paper.

Acknowledgements

Authors thanks to anonymous referees and editor for their valuable contributions on this paper.

References

[1] K.P. Sharp, Stochastic differential equations in finance, Appl. Math. Comput. 39 (3) (1990) 207–224.
[2] F. Antonelli, Stability of backward stochastic differential equations, Stochastic Process. Appl. 62 (1) (1996) 103–114.
[3] A.D. Irving, T. Dewson, Determining mixed linear-nonlinear coupled differential equations from multivariate discrete time series sequences, Physica D 102 (1–2) (1997) 15–36.

[4] X. Jin, S. Deng, Existence and uniqueness of optimal consumption and portfolio rules in a continuous-time finance model with habit formation and without short sales, J. Math. Econ. 28 (2) (1997) 187–205.

[5] B. Ganesh, P.P. Muthukumar, Controllability study on fractional order impulsive stochastic differential equation, IFAC-Papers OnLine 4 (1) (2016) 516–521.

[6] A.A. Samarskii, Economical difference schemes for parabolic equations with mixed derivatives, USSR Comput. Math. Math. Phy. 4 (4) (1964) 182–191.

[7] B. Decardi-Nelson, J. Liu, Robust Economic Model Predictive Control with Zone Control, IFAC-Papers OnLine 54 (3) (2021) 237–242.

[8] G. Adomian, On the Modeling and Analysis of a National Economy, IFAC Proc. Vol. 16 (7) (1983) 189–196.

[9] C. Maffezoni, G. Magnani, L. Marcocci, Computer Aided Modelling of Large Power Plants, IFAC Proc. Vol. 17 (3) (1984) 1–9.

[10] V.G. Ivancevic, Adaptive-Wave Alternative for the Black-Scholes Option Pricing Model, Cognit. Comput. 2 (2010) 17–30.

[11] Y.Q. Chen, Y.H. Tang, J. Manafian, H. Rezazadeh, M.S. Osman, Dark wave, rogue wave and perturbation solutions of Ivancevic option pricing model, Nonlinear Dyn. 105 (2021) 2539–2548.

[12] W. Gao, H.F. Ismael, A.M. Husien, H. Bulut, H.M. Baskonus, Optical Soliton solutions of the Nonlinear Schrödinger and Resonant Nonlinear Schrödinger Equation with Parabolic Law, Appl. Sci. 10 (1) (2020) 219.

[13] J.L.G. Guirao, H.M. Baskonus, A. kumar, M.S. Rawat, G. Yel, Complex Soliton Solutions to the (3 + 1)-Dimensional B-type Kadomtsev-Petviashvili-Boussinesq Equation, Symmetry 12 (1) (2020) 17.

[14] H.F. Ismael, H. Bulut, H.M. Baskonus, Optical soliton solutions to the Fokas-Lenells equation via sine-Gordon expansion method and (m + G'/G)-expansion method, Pramana-J. Phys. 94 (35) (2020) 1–9.

[15] C. Dai, Y. Wang, Periodic Structures Based on Variable Separation Solution of the (2 + 1)-Dimensional Boiti-Leon-Pempinelli Equation, Chaos Solitons Fract. 39 (2009) 350–355.

[16] A. Ciancio, G. Yel, A. Kumar, H.M. Baskonus, E. Ilhan, On the complex mixed dark-bright wave distributions to some conformable nonlinear integrable models, Fractals 30 (1) (2022) 2240018 (14 pages).

[17] A. Kumar, E. Ilhan, A. Ciancio, G. Yel, H.M. Baskonus, Extractions of some new travelling wave solutions to the conformable Date-JimboKashiwara-Miwa Equation, Aims Math. 6 (5) (2021) 4238–4264.

[18] Y.M. Li, H.M. Baskonus, A.M. Khudhur, Investigations of the Complex Wave Patterns to the Generalized Calogero-Bogoyavlenskii-Schiff Equation, Soft. Comput. 25 (10) (2021) 6999–7008.

[19] H.M. Baskonus, Dark and trigonometric soliton solutions in asymmetrical Nizhnik-Novikov-Veselov equation with (2 + 1)-dimensional, Int. J. Optimiz. Control Theor. Appl. (IJOCTA) 11 (1) (2021) 92–99.

[20] A.R. Seadawy, M. Arshad, D. Lu, Stability analysis of new exact traveling-wave solutions of new coupled KdV and new coupled ZakharovKuznetsov systems, Eur. Phys. J. Plus 132 (162) (2017) 1–10.

[21] A. Govindarajan, B.A. Malomed, A. Mahalingam, A. Uthayakumar, Modulational Instability in Linearly Coupled Asymmetric Dual-Core Fibers, Appl. Sci. 7 (7) (2017) 645.

[22] A.R. Seadawy, Modulation instability analysis for the generalized derivative higher order nonlinear Schrödinger equation and its the bright and dark soliton solutions, J. Electromagn. Waves Appl. 31 (14) (2017) 1353–1362.

[23] K.K. Ali, R. Yilmazer, H.M. Baskonus, H. Bulut, Modulation instability analysis and analytical solutions to the system of equations for the ion sound and Langmuir waves, Phys. Scr. 95 (6) (2020) 065602.

[24] V.G. Ivancevic, T.T. Ivancevic, Sine-Gordon Solitons, Kinks and Breathers as Physical Models of Nonlinear Excitations in Living Cellular Structures, arXiv:1305.0613v1, 2013.

[25] T.A. Sulaiman, H. Bulut, Optical solitons and modulation instability analysis of the (1 + 1)-dimensional coupled nonlinear Schrödinger equation, Commun. Theor. Phys. 2 (2020) 25003.

[26] A.R. Seadawy, Stability analysis solutions for nonlinear three-dimensional modified Korteweg-de Vries-Zakharov-Kuznetsov equation in a magnetized electron-positron plasma, Physica A 455 (2016) 44–51.

[27] W. Gao, H.F. Ismael, H. Bulut, H.M. Baskonus, Instability modulation for the (2+ 1)-dimension paraxial wave equation and its new optical soliton solutions in Kerr media, Phys. Scripta 95 (3) (2020) 035207.

[28] R.M. Jena, S. Chakraverty, D. Baleanu, A novel analytical technique for the solution of time-fractional Ivancevic option pricing model, Physica A 550 (124380) (2020).

[29] Z. Yan, Vector financial rogue waves, Phys. Lett. A 375 (48) (2011) 4274–4279.

[30] S.O. Edeki, O.O. Ugbebor, O. Gonzalez-Gaxiola, Analytical solutions of the Ivancevic option pricing model with a nonzero adaptive market potential, Int. J. Pure Appl. Math. 115 (1) (2017) 187–198.

[31] F. Dusunceli, New Exact Solutions for Generalized (3 + 1) dimensional Shallow Water-Like (SWL) Equation, Appl. Math. Nonlin. Sci. 4 (2) (2019) 365–370.

[32] G. Yel, T. Akturk, A New Approach to (3 + 1) Dimensional Boiti-Leon-Manna-Pempinelli Equation, Appl. Math. Nonlin. Sci. 5 (1) (2020) 309–316.

[33] S.S. Ray, New soliton solutions of conformable time fractional Caudrey-Dodd-Gibbon-Sawada-Kotera equation in modeling wave phenomena, Mod. Phys. Lett. B 33 (18) (2019) 1950202.

[34] E.I. Eskitascioglu, M.B. Aktas, H.M. Baskonus, New Complex and Hyperbolic Forms for Ablowitz-Kaup-Newell-Segur Wave Equation with Fourth Order, Appl. Math. Nonlin. Sci. 4 (1) (2019) 105–112.

[35] A. Antuña, J.L.G. Guirao, M.A. López, On the perturbations of maps obeying Shannon-Whittaker-Kotel'nikov's theorem generalization, Adv. Difference Eqs. 378 (2021) (2021) 1–12.

[36] A. Antuña, J.L.G. Guirao, M.A. López, Shannon-Whittaker-Kotel'nikov's theorem generalized, MATCH J. Math. Chem. 58 (5) (2020) 893–905.

[37] N.Y. Aksoy, The Solvability of First Type Boundary Value Problem for a Schrödinger Equation, Appl. Math. Nonlin. Sci. 5 (1) (2020) 211–220.

[38] H. Bulut, A.N. Akkilic, B.J. Khalid, Soliton solutions of Hirota equation and Hirota-Maccari system by the (m + 1/G')-expansion method, Adv. Math. Models Appl. 6 (1) (2021) 22–30.

[39] K.S. Al-Ghafri, H. Rezazadeh, Solitons and other solutions of (3 + 1)-dimensional space-time fractional modified KdV-Zakharov-Kuznetsov equation, Appl. Math. Nonlin. Sci. 4 (2) (2019) 289–304.

[40] G. Yel, C. Cattani, H.M. Baskonus, W. Gao, On the complex simulations with dark-bright to the Hirota-Maccari system, J. Comput. Nonlinear Dyn. 16 (6) (2021) 061005.

[41] T.A. Sulaiman, H. Bulut, The new extended rational SGEEM for construction of optical solitons to the (2 + 1)-dimensional Kundu-Mukherjee-Naskar model, Appl. Math. Nonlin. Sci. 4 (2) (2019) 513–522.

[42] A. Antuña, J.L.G. Guirao, M.A. López, Pseudo-radioactive decomposition through a generalized Shannon's recomposition theorem, MATCH Commun. Math. Comput. Chem. 72 (2) (2014) 403–410.